Revista Brasileira de Ciência do Solo
ISSN: 0100-0683
revista@sbcs.org.br
Sociedade Brasileira de Ciência do Solo
Brasil

Alves, Marcelo Rodrigo; Demattê, José A. M.; Silva Barros, Pedro Paulo
Multiple Geotechnological Tools Applied to Digital Mapping of Tropical Soils
Revista Brasileira de Ciência do Solo, vol. 39, núm. 5, mayo, 2015, pp. 1261-1274
Sociedade Brasileira de Ciência do Solo
Viçosa, Brasil

Available in: http://www.redalyc.org/articulo.oa?id=180242692003

How to cite
Complete issue
More information about this article
Journal's homepage in redalyc.org

Scientific Information System
Network of Scientific Journals from Latin America, the Caribbean, Spain and Portugal
Non-profit academic project, developed under the open access initiative

Comissão 1.3 - Pedometria

MULTIPLE GEOTECHNOLOGICAL TOOLS APPLIED TO DIGITAL MAPPING OF TROPICAL SOILS

Marcelo Rodrigo Alves[(1)], José A. M. Demattê[(2)*] and Pedro Paulo Silva Barros[(3)]

[(1)] Universidade do Oeste Paulista, Presidente Prudente, São Paulo, Brasil.
[(2)] Universidade de São Paulo, Escola Superior de Agricultura Luiz de Queiroz, Departamento de Ciência do Solo, Piracicaba, São Paulo, Brasil.
[(3)] Universidade de São Paulo, Escola Superior de Agricultura Luiz de Queiroz, Departamento de Engenharia de Biossistemas, Piracicaba, São Paulo, Brasil.
* Corresponding author.
E-mail: jamdemat@usp.br

ABSTRACT

In recent years, geotechnologies as remote and proximal sensing and attributes derived from digital terrain elevation models indicated to be very useful for the description of soil variability. However, these information sources are rarely used together. Therefore, a methodology for assessing and specialize soil classes using the information obtained from remote/proximal sensing, GIS and technical knowledge has been applied and evaluated. Two areas of study, in the State of São Paulo, Brazil, totaling approximately 28.000 ha were used for this work. First, in an area (area 1), conventional pedological mapping was done and from the soil classes found patterns were obtained with the following information: a) spectral information (forms of features and absorption intensity of spectral curves with 350 wavelengths -2,500 nm) of soil samples collected at specific points in the area (according to each soil type); b) obtaining equations for determining chemical and physical properties of the soil from the relationship between the results obtained in the laboratory by the conventional method, the levels of chemical and physical attributes with the spectral data; c) supervised classification of Landsat TM 5 images, in order to detect changes in the size of the soil particles (soil texture); d) relationship between classes relief soils and attributes. Subsequently, the obtained patterns were applied in area 2 obtain pedological classification of soils, but in GIS (ArcGIS). Finally, we developed a conventional pedological mapping in area 2 to which was compared with a digital map, ie the one obtained only with pre certain standards. The proposed methodology had a 79 % accuracy in the first categorical level of Soil Classification System, 60 % accuracy in the second category level and became less useful in the categorical level 3 (37 % accuracy).

Keywords: soil spectral behavior, terrain features, remote sensing.

Received for publication on July 11, 2014 and approved on May 29, 2015.
DOI: 10.1590/01000683rbcs20140410

CC BY

RESUMO: *MÚLTIPLAS FERRAMENTAS TECNOLÓGICAS NO MAPEAMENTO DIGITAL EM SOLOS TROPICAIS*

Nos últimos anos, geotecnologias como sensoriamento remoto, espectrorradiometria próxima e atributos do terreno derivados de modelos digitais de elevação são muito úteis para a descrição da variabilidade do solo. No entanto, essas fontes de informação são raramente usadas em conjunto. Por este motivo, uma metodologia para atribuir e especializar classes de solos utilizando-se de informações obtidas com sensoriamento remoto/proximal, geoprocessamento e conhecimento técnico foi aplicada e avaliada. Duas áreas de estudo, localizadas no Estado de São Paulo, Brasil, e totalizando aproximadamente 28.000 ha, foram utilizadas. Primeiramente, em uma área (Área 1), realizou-se o mapeamento pedológico convencional e a partir das classes de solos encontradas foram obtidos padrões com as seguintes informações: a) informações espectrais (características de formas e intensidade de absorção das curvas espectrais com comprimentos de onda de 350 - 2500 nm), de amostras de solo coletadas em pontos específicos nas áreas (de acordo com cada classe de solo); b) Obtenção de equações de determinação de atributos químicos e físicos do solo a partir da relação entre os resultados obtidos em laboratório, pelo método convencional, dos teores dos atributos químicos e físicos com os dados espectrais; c) classificação supervisionada de imagens Landsat TM 5, a fim de detectar alterações no tamanho das partículas do solo (textura do solo); d) relação entre as classes de solos e atributos do relevo. Posteriormente, os padrões obtidos foram aplicados na Área 2 a fim de obter-se a classificação pedológica destes solos, porém em ambiente SIG (ArcGis). Para finalizar, ainda foi realizado na Área 2 o mapeamento pedológico convencional para então comparar o mapa convencional com o mapa digital, ou seja, aquele obtidos apenas com padrões pré-determinados. A metodologia proposta teve expressivo resultado no primeiro nível categórico do Sistema de Classificação de Solos (79 % de acerto), um desempenho satisfatório até o segundo nível categórico (60 % de acerto) e tornou-se menos útil no nível categórico 3 (37 % de precisão).

Palavras-chave: comportamento espectral do solo, atributos do terreno, sensoriamento remoto.

INTRODUCTION

People are becoming aware that soil resources are not renewable in the time-scale of human generations and, consequently, are limited. Thus, the need for information leading to greater knowledge of soil use becomes more imperative. This knowledge is essential for maintaining populations, not only in terms of food production and raw materials, but also as a subsidy for urban development and environmental studies, among others. Most knowledge is obtained through what is known as pedological inventories or pedological surveys, which are nothing more than the examination and identification of soils, the establishment of their geographical boundaries, representation and description of soils on the map, and interpretation of their purpose.

In Brazil, the first soil surveys were carried out during the 1930s, with the objective of characterizing, identifying, and assessing potential sites for irrigation projects downstream from public dams in the Brazilian Northeast. However, the greatest boost in soil surveys occurred in the late 1940s, when the Ministry of Agriculture established the National Commission of Agronomic Research (Centro Nacional de Ensino e Pesquisas Agronômicas - CNEPA) to study soils in the vast territory of Brazil. Soil studies involved classification, fertility, management, and conservation, in addition to the basic research of physical, chemical, and mineralogical characterization of soils. There was an extensive program of soil surveys on the exploratory level of recognition, which for three decades produced most of the pedological information available today. Currently, around 35 % of Brazilian soils (17 states and the federal district) are mapped on medium to undetailed scales (1:100,000 to 1:600,000) and complete coverage of the country at the exploratory level, on undetailed scales (1:1,000.000 to 1:5,000.000) (Santos, 2007). From the mid-1980s on, soil surveys in Brazil have been practically stagnant, mainly due to lack of incentives from the government, along with poor working conditions (problems with food, fresh water, road traffic conditions, cars, and medical assistance), the slow pace of officials, costly fieldwork, and difficulties in laboratory analyses.

Although surveys performed on the exploratory/schematic level are not considered highly valuable due to poor detail, they were very important for establishing public policies that gave rise to cartographic resources to develop land use and support the potential of land use on the regional level. In general, for all other purposes that require detailed soil surveys, Brazil is a country wholly deficient with regard to soil surveys (Oliveira, 1999).

The continuity of implementing surveys, at any level, depends on the use of technological advances, especially advances in soil mapping. Otherwise,

efficient development of detailed maps may be hindered. The aim of computer use is not to replace the conventional method of soil surveys, but to assist and optimize the work.

Many multidisciplinary studies show the efficiency of technological tools in soil studies, for example, orbital spectroradiometry. Although the soil is usually covered with vegetation and the soil surface is not visible, some soil properties can be directly assessed by their spectral signatures (Rossiter, 2005). Some of these notable soil properties are moisture (Jackson et al., 1996), physical and chemical characteristics (Odeh and McBratney, 2000), and salts (Metternicht and Zinck, 2003). Moreover, integrated use of geostatistical techniques with remote sensing data for spatialization is important (Stein et al., 1998).

Studies on spectroradiometry show a strong relationship between spectral responses and soil properties, such as cation exchange capacity, organic carbon, Fe oxides, and clay (Chang et al., 2001; Shepherd and Walsh, 2002; Franceschini et al., 2013; Nanni and Demattê, 2006; Demattê et al., 2014a). In fact, this led Demattê et al. (2004a) to use a spectroscopy information to aid in pedological mapping. Afterwards, Fiorio et al. (2014) suggest the use of spectral sensors for the aid of field work in pedological maps. In addition to laboratory or field spectroscopy, we can also gather information from space (using Landsat data) as a valuable strategy (Demattê et al., 2009).

Another example of geotechnology applied to soil studies is the use of numerical models of land and their primary and secondary derivatives (McBratney et al., 2003), which are applied in the characterization and delineation of mapping units (McKenzie et al., 2000). The relationship of topographic features to soil properties was proved by Milne (1935); however, this relationship has been used more significantly in recent years, mainly due to the technological progress that facilitated access to powerful computers, as well as tools such as the Geographic Information System (GIS) and Global Positioning System (GPS) (Rossiter, 2005).

Although these techniques have proven helpful, few studies joined geoprocessing techniques, remote sensing (ground and orbital), relief analysis, field observations, and technical knowledge in a concise, accurate, and scientific way in soil surveys. However, basic studies such as morphopedology, photopedology, remote/proximal sensing, and geoprocessing focus on one unique technique, and are not linked. Nothing more logical than integrating the information generated, resulting in a more accurate and less costly soil map, which is generated more quickly and covers larger areas.

This study is based on the hypothesis that it is possible to determine a method that allows characterization, discrimination, and spatialization of soil classes, integrating the information obtained from remote/proximal sensing and geoprocessing, since these techniques are complementary. We expect that using each several remote sensing techniques will achieve a better soil map than traditional methods. Thus, the main objective is to generate a technique for developing a highly-detailed level of soil mapping with the integration of geotechnologies.

MATERIAL AND METHODS

Study site

The study site consists of two areas (1 and 2) of sugarcane *(Saccharum spp)* cultivation, each composed of several non-continuous plots. These sites are located in the northeastern region of São Paulo, involving several municipalities, such as São Carlos, Araraquara, and Ibaté, among others (21º 16' 59" S/48º 39' 31" W and 21º 45' 19" S/48º 6' 2" W). The areas together cover approximately 28,000 ha, with 15,000 ha in area 1 and 13,000 ha in area 2. The region ranges from 450 - 900 m above sea level, and the climate is mesothermal (dry winters and wet summers). Annual average rainfall ranges from 1,000 - 1,800 mm, and annual average temperature is around 20 ºC. Lithology is represented mainly by the Serra Geral, Botucatu, and Pirambóia Formation (São Bento Group) and covered by the Serra de Santana Formation and others (Taubaté Group). The rocks of the Serra Geral Formation are volcanic, mainly basaltic. The rocks of the Botucatu Formation are wind sandstones, and the rocks of the Pirambóia Formation are composed of sandstones originating from fluvial deposits and flood plains (Bistrichi et al., 1981).

Methodology

The methodology proceeded in three stages: (a) determination of soil patterns in part of the studied area; (b) application of patterns obtained from stage "a" in a second unknown area; and (c) validation of soil mapping. We used wholly geotechnological patterns to create a digital map of the soil. We validated the digital map by cross-tabulating the digital and conventional soil maps with a conventional soil map of the unknown area.

Stage 1 - Determination of soil patterns

This stage was performed in area 1. The patterns of soil profiles were extracted from a semi-detailed soil map. The map was created by the conventional method, with 300 sampling points distributed according to the transection method. The samples were collected at three different depths (0.00 - 0.20, 0.40 - 0.60 and 0.80 - 1.00 m) for a total of 900 soil

samples. In addition, 40 complete soil profiles were described and laboratory analyses were made to determine the following soil properties: sand, silt, clay, Ca^{2+}, Mg^{2+}, Al^{3+}, and H + Al (Embrapa, 2013) in the soil exchange complex, and total contents of Fe, Ti, Si, and Al (Camargo, 1986). The sampling points were georeferenced with GPS. Figure 1 shows the activities in stage 1.

Spectral data acquisition at the laboratory level

The spectral data for the 900 soil samples collected from area 1 were obtained by the portable Fieldspec Pro sensor (ASD Inc., Boulder, Colorado, USA), within the 350 - 2,500 nm wavelength range, following the method described by Bellinaso et al. (2010). The spectral data was processed after measurement to smooth the spectral curves through application of the Savitzky-Golay method, with the 2^{nd} polynomial order and a 9-point window (Savitzky and Golay, 1964). Subsequently, the spectral data were processed following the method of Nanni and Demattê (2006), with 22 bands (B1, B2…B22) and 13 heights (H1, H2...H13).

Spectral information and soil properties determined by conventional analysis were joined in a data matrix. A mathematical procedure was applied to deduce multiple regression equations, which allowed estimation of soil properties from the soil spectral data. The equations were used in area 2 (unknown area). The multiple regression equations were calculated to quantify 19 physical and chemical soil properties.

Multiple linear regression analysis was performed with SPSS 11.0 software using the stepwise method (Glantz and Slinker, 1990). The equations were evaluated according to R^2, RMSE, and e_m indexes (Kobayashi and Salam, 2000; Brown et al., 2006; Wolschick et al., 2007).

Evaluation of pure spectral curves

The spectral curves obtained for each sampling point at different depths were correlated with a spectral library (Bellinaso et al., 2010) in order to sort and collate the spectra by soil class. Subsequently, each class obtained was analyzed in terms of form, intensity, and absorption of their respective groups of spectral curves (Demattê et al., 2002, 2014b), to be used as a pattern for the group of curves obtained in area 2.

Satellite images and supervised classification

Five satellite images were taken from Landsat 5 (Thematic Mapper sensor), WRS 220/075, dated 08/17/2002, 08/14/2004, 08/17/2005, 05/09/2006, 08/09/2007, with six spectral bands (B1: 450 - 520; B2: 520 - 600; B3: 630 - 690; B4: 760 - 900; B5: 1,550 - 1,750; and B6: 2,080 - 2,350 nm), a spatial

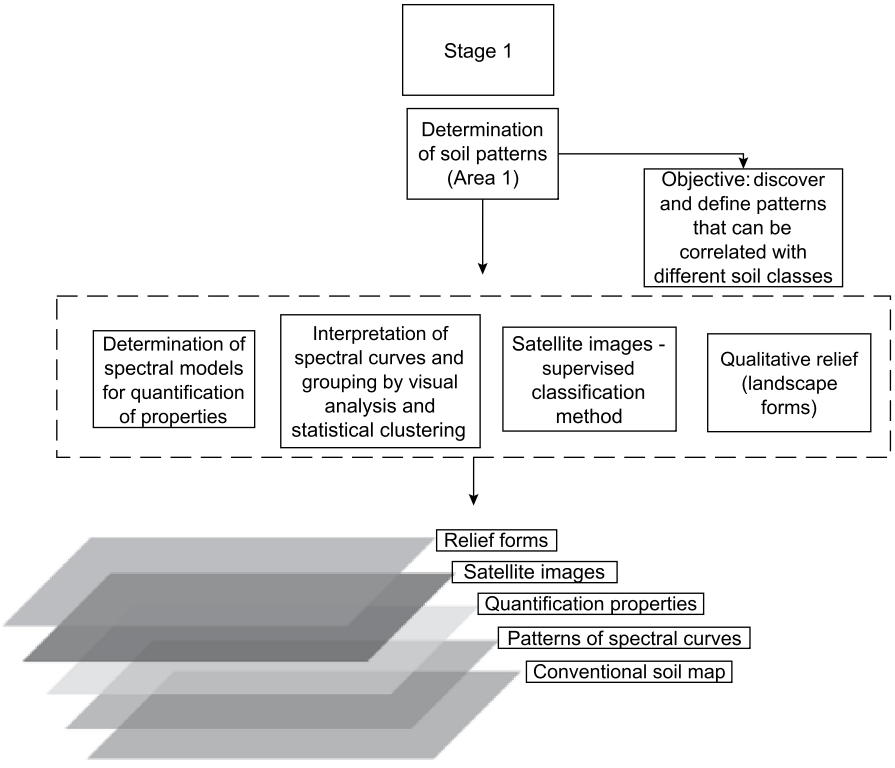

Figure 1. Flowchart of activities in stage 1.

resolution of 30 m, and average altitude of orbit of 705 km. The reason the images were obtained in different years is that in large commercial plantations of sugar cane, soil preparation for crop renewal (which implies exposed soil), materializes through installments over the years, that is, each year soil tillage and preparation is carried out on a percentage of the area. This system forms a five-year cycle on average for the area under study, which means that the area prepared this year will only be prepared again in five years.

The images were registered according to Mitishita et al. (1988). For the purpose of maintaining the pixel value as similar as possible to the original value, the method called "nearest neighbor interpolation" was used, correcting only distortions in scale, and displacement or rotation between image and land projection (Crósta, 1992). All procedures for land registration were performed in the ENVI 4.3 program (RSI, 2006). Afterwards, the digital numbers of the image were processed for apparent reflectance (AR) (Antunes et al., 2003) to be converted to images of surface reflectance (Vermote et al., 1997) in the 6S program (Second Simulation of the Satellite Signal in the Solar Spectrum).

To separate areas with vegetation from those with exposed soil, we performed the Linear Model of Spectral Mixture - LMSM (Shimabukuro and Smith, 1991) and the Normalized Difference by Vegetation Index - NDVI (Rouse et al., 1974; Deering et al., 1975).

Thus, in each of the images (surface reflectance), sampling points are overlapped and only those with exposed areas of soil were preserved and used as a reference for later supervised classification. In each of the selected points, clay content in the surface layer was observed and rated in one of the following classes: sandy (<150 g kg^{-1}), sandy medium (150 - 250 g kg^{-1}), medium loamy (250 - 350 g kg^{-1}), clay (350 - 600 g kg^{-1}), and very clay (>600 g kg^{-1}). Thus, the spectral information of the set of points belonging to each class is grouped in a library.

Next, a supervised classification procedure was applied to the images using the algorithm of Gaussian distribution by maximum likelihood (Rodrigues et al., 2007).

Derivation of terrain features

Digital contour lines with vertical equidistance of 20 m were used to derive a digital elevation model (DEM) for the site under study. From this, primary (slope and plan curvature) and secondary (compound topographic index (CTI) and potential drainage density (PDD)) terrain features were calculated according to Moore et al. (1993), Dobos et al. (2000), Shary et al. (2002), Gessler et al. (1995), and McBratney et al. (2003).

The spatial maps of the primary and secondary terrain features were tabulated in the ArcGIS 9.3 software, with the detailed soil map of area 1. The objective was to correlate soil classes with terrain information to use this as additional information for delimitation of the mapping unit in the next stage.

Stage 2 - Applying patterns in area 2

In this stage, the main objective was to use all patterns and knowledge acquired in stage 1 to determine a digital soil map in an unknown area (area 2).

Field examination, collection, and processing of soil samples

Initially, area 2 was studied to recognize the general characteristics of the site. Satellite imaging and elevation data were used as field support. Afterwards, toposequences of 225 sampling points were collected at three depths (0.00 - 0.20, 0.40 - 0.60, and 0.80 - 1.00 m) and analyzed for chemistry and spectra.

Digital soil mapping based on patterns of stage 1

Quantification of soil properties by spectral models

From the soil spectral data of area 2, each physical and chemical property was quantified using the multiple regression models deduced from data of area 1, which allowed tabulation of soil properties estimated for each of the 225 soil samples. Additional information was provided by color measurement of surface and subsurface layers of wet soil samples in the laboratory using the colorimetric method.

Analysis of spectral curves

The spectral curves from each sampling point were visually compared to the patterns identified in stage 1 and assigned to a soil group. Thus, the soil class of greatest similarity to each sampling point was tabulated with soil properties estimated from the spectral data and used in final classification of each soil sample.

Cluster analysis

The soil samples collected in area 2 were classified in homogeneous groups in cluster analysis (Demattê et al., 2004a), which was based on spectral information for each soil sample. Therefore, cluster analysis compared all sampling points that determined similar groups of curves. The clustering strategy used was Average Linkage, which allowed identification of sequential, hierarchical, and non-overlapping groups (Sneath and Sokal, 1973). The similarity coefficient applied was Euclidean distance, and it was implemented in the software SPSS 11.0.

Soil classification based on all information acquired

After all data were collected, the procedure for final soil classification of each sampling point was: (1) soil samples were grouped based on visual patterns of spectral curves; (2) quantitative data of physical and chemical soil properties estimated from models deduced in stage 1 were tabulated, and color measurements were tabulated with other soil properties; and (3) the tabulated data were used to fit the results of cluster analysis, and each point was properly classified. The key-process was similar to interpretation of soil analysis in the traditional soil mapping method; however, additional properties were analyzed: (4) in situations where this information was not enough to classify a sampling point, we observed the cluster analysis of the most similar sample that had been classified. This soil class was then assigned to the unclassified sample; and (5) other data that supported the decision for the final soil classification were terrain features, such as slope and elevation. Each point was related to the relief features using a geographical information system. Based on patterns of stage 1, the possibility of occurrence of a certain soil class at a point was indicated based on terrain features. This information was considered in the final decision.

Soil classification followed the SiBCS (Brazilian Soil Classification System, Embrapa, 2013) and was also related with the USDA (2010) along the text and tables.

Spatial analysis and delineation of the soils (Satellite imaging supervised classification)

Supervised classification was used to characterize the surface of the study site through orbital information, based on the patterns obtained in stage 1. Thus, complementary information was obtained, not to classify the soil, but to complement the database to make decisions based on the delimitation of mapping units.

Relief analysis

Similar to traditional soil mapping, contour lines were mainly delimited with vertical equidistance of 20 m, and some observations were made in the slope map of the study site. In example 1, the cluster and spreadsheet analyses were sufficient to classify the soil. In example 2, the spreadsheet was not clear enough and the final decision was made based on cluster analysis. In example 3, the final decision was made based on the position of the point in the relief (Figure 2).

Delimitation of soils

All information obtained (classification of soil samples, terrain features, and supervised classification of satellite imaging) was organized in a database using the ArcGIS 9.3 software. Thus, information layers were used in the delimitation of mapping units (Figure 3), which was performed manually by digitalizing the vectors (polygons). Finally, soils of area 2 were obtained.

Stage 3 - Validation of the digital soil map

The digital soil map obtained in area 2 was validated using the cross-tabulation method, which correlated with the conventional soil map on a detailed level (1:20,000) developed in this study. This was carried out in two ways: (a) the soil class of each sampling point in the conventional soil map was compared with the soil class obtained from the digital soil mapping approach, and (b) cross-tabulation was compared with spatial information obtained from both approaches (conventional and digital) at the level of the mapping unit.

In both cases, the soil was first classified to the 3rd category level in the SiBCS (Brazilian Soil Classification System), and texture classification was added, for example a *Latossolo Vermelho Distrófico argiloso* (Embrapa, 2013) - Clayey Rhodic Hapludox (USDA, 2010). We used in the text Brazilian and USDA soil classification. Afterwards, the soil class was decomposed, and each criterion was evaluated separately. The characteristics evaluated were the same used in classifying the soil up to the 3rd category level and texture class: (a) soil class; (b) soil color classified in three types (red, yellowish red, and yellow), as color determination in the colorimeter (Munsell color system) was given in hue values with decimals (continuous variable); these values were classified as yellow if the measurements were above 7.5 YR, classified as yellowish red if color data were from 7.5 YR to 2.5 YR, and classified as red if values were below 2.5 YR; (c) soil fertility analysis, based on three main criteria: base saturation higher than 50 % (eutrophic), base saturation lower than 50 % (dystrophic), and Al saturation higher than 50 %; (d) Fe oxide contents in the soil were evaluated observing results of extraction by sulfuric acid; values higher than 180 g kg^{-1} were considered iron rich and classified as ferric (higher than 180 g kg^{-1} of Fe oxides); and (e) texture classes as described above.

Cross-tabulations resulted in confusion matrices, and indexes of classification accuracy were derived from these matrices. The indexes calculated were overall accuracy and the Kappa index (Story and Congalton, 1986; Congalton and Green, 1999).

Classification performance which was evaluated using the ranges proposed by Fonseca (2000) for the Kappa coefficient (K), were: $K<0$, Very poor; $0<K\leq0.2$, poor; $0.2<K\leq0.4$, Reasonable; $0.4<K\leq0.6$, Good; $0.6<K\leq0.8$, Very good; and $0.8<K\leq1.0$, Excellent.

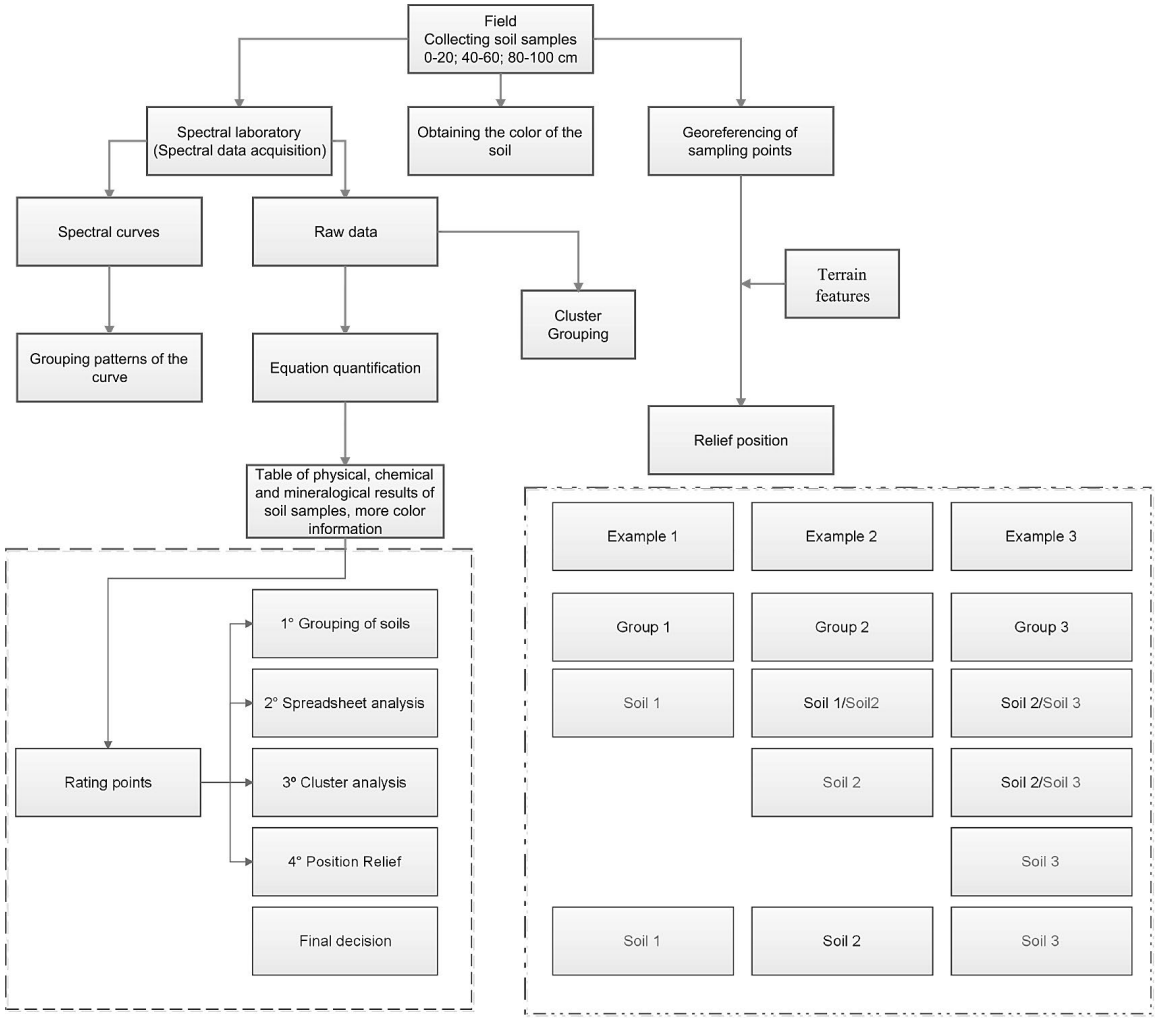

Figure 2. Flowchart illustrating the work sequence.

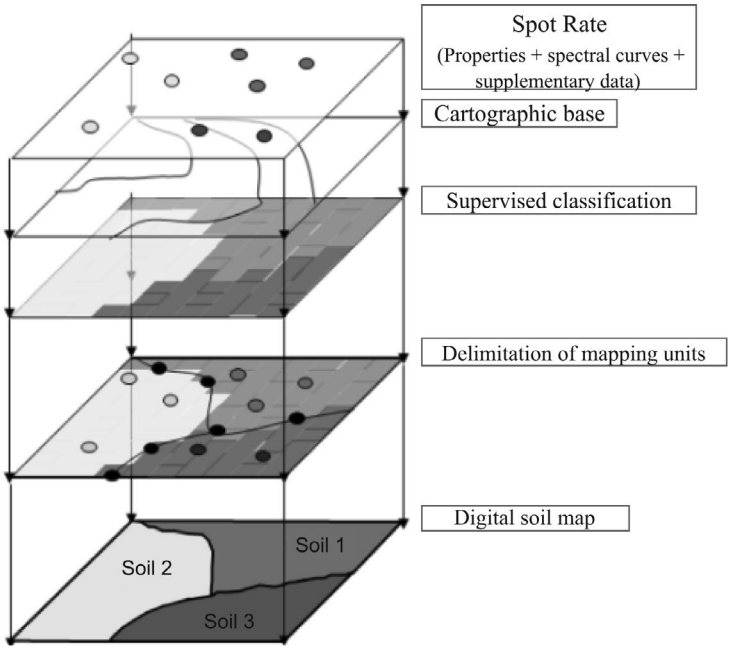

Figure 3. Illustration of the arrangement of information layers that composed the digital soil map.

RESULTS AND DISCUSSION

Quantification of Soil Properties

Multiple regression equations were fitted to predict values of 19 soil properties from their spectral response (Table 1). Of these, five exhibited R^2 greater than 0.59, namely, Fe_2O_3, Al_2O_3, clay, Ki, and SiO_2. Fe_2O_3 stood out at 0.82. Our results corroborate those obtained by Janik et al. (1998), Nanni and Demattê (2006), Demattê et al. (2004a), and Demattê et al. (2014a). It is notable that high coefficients for the physical properties such as sand, clay, and Fe_2O_3 were achieved, since these parameters have a significantly greater influence on the spectral response of the soil.

The sum of bases (SB), cation exchange capacity (CEC), and base saturation (V) showed the following values for R^2: 0.44, 0.46, and 0.29, respectively, in contrast with Nanni and Demattê (2001), Dunn et al. (2002), and Demattê et al. (2004a), who found values of R^2 greater than 0.74 for these properties. However, such properties often show coefficients with values lower than 50 % (Demattê and Garcia, 1999). Few studies have been carried out to explain the influence of chemical properties on the spectral response of soils (Demattê et al., 2004a), possibly due to the dynamic nature of soil reactions.

The estimated values were compared with values determined in conventional laboratory analysis for the purpose of verifying the possibility of using the data on soil fertility estimated by the equations, especially the data used as criteria to achieve the 3rd category level in soil classification. Values obtained in the equations tended to overestimate dystrophic soils and underestimate eutrophic and aluminic ones (Table 2). However, the percentage of accuracy exceeded 76 %, even reaching 98 %, as in the example of m groups.

Spectral curves as indicators for soil classification

The analyses of spectral curves for soil samples collected in area 1, which gave rise to the patterns applied in area 2, allowed determination of three distinct groups (Figure 4). The first group was characterized mainly by the presence of deep, well-drained soils, with texture ranging from sandy-clayey to clayey, especially in Latosols

Table 2. Matrix of accuracy and error of values determined in the laboratory by conventional soil analyses and values estimated by multiple regression equations for the variables base saturation (V), aluminum saturation (m), and aluminum exchangeable (Al^{3+})

		Estimated values[1]		
	V (%)[3]	≤50	>50	Total
Determined values[2]	≤50	454	44	498
	>50	103	24	127
	Total	557	68	625[5]
	Overall accuracy =		0.76	
	m (%)[4]	≤50	>50	
	≤50	610	0	610
	>50	13	2	15
	Total	623	2	625
	Overall accuracy =		0.98	
	Al^{3+} ($cmol_c\ kg^{-1}$)	<4	≥4	
	<4	515	2	517
	≥4	99	9	108
	Total	614	11	625
	Overall accuracy =		0.84	

[1] Values estimated by multiple regression equations; [2] Values determined in the laboratory by conventional soil analysis; [3] Base saturation (BS/CEC × 100); [4] Aluminum saturation (Al/Al + BS) × 100; [5] Number of total samples at three depths (0.00 - 0.20, 0.40 - 0.60, and 0.80 - 1.00 m).

Table 1. Multiple regression equations developed from soil reflectance and obtained at ground level

Property	Equation[1]	R^2	RMSD[2]	ME[3]
Clay ($g\ kg^{-1}$)	Clay = 344.485 + 21,560.041 H2 + 1,973.068 B7 - 3,895.359 B21 - 10,231.5 H5 - 30,019.3 B3 + 21,789.511 B5 + 6,386.753 B4 + 2,877.608 H8 + 6,253.900 B13 – 4,353.122 B16	0.75	63.8	20.65
OM[4] ($g\ kg^{-1}$)	OM = 24,887 - 160.911 H4 – 91,569 B21 - 185.125 H3 - 282.773 H5	0.32	4.16	37.88
SB[5] ($mmol_c\ kg^{-1}$)	$SB = 10^{(1,581 + 27,440\ H8 – 48,716\ H5 + 20,635\ H7 – 7,646\ H4 – 12,603\ H1 – 2,866\ B22)}$	0.44	10.67	44.57
CEC[6] ($mmol_c\ kg^{-1}$)	$CEC = 10^{(1,181 - 8,391\ H6 + 13,141\ H8 + 5,667\ H9 – 16,127\ H5 – 2,748\ B4 + 4,860\ B7 – 3,017\ B19)}$	0.46	12.69	20.12
Fe_2O_3 ($g\ kg^{-1}$)	$Fe_2O_3 = 10^{(1,242 + 30,182\ H7 + 8,823\ H11 - 9,005\ H9 - 5.283\ H4 - 5,957\ B2 + 5,860\ H3)}$	0.82	3.53	24.13
SiO_2 ($g\ kg^{-1}$)	$SiO_2 = 10^{(1,291 – 6,225\ B22 + 1,396\ B5 – 4,150\ H11 – 2,955\ H13 + 2,926\ B14)}$	0.59	2.12	20.07
Al_2O_3 ($g\ kg^{-1}$)	$Al_2O_3 = 10^{(1,373 - 5,714\ B20 - 2,883\ H2 + 6,810\ B13 - 4,254\ B17)}$	0.81	2.21	16.90
Ki	Ki = 1,391 - 15,875 H11 + 10,696 H2 + 15,438 H3 - 25,592 H9 + 26,745 H7 + 2,890 B18	0.61	0.19	13.40

[1] Bands and heights selected; [2] Root mean square deviation; [3] Mean error; [4] Organic matter; [5] Sum of bases (Ca+Mg+K); [6] Cation exchange capacity (BS+H+Al).

(Oxisols). These soils show spectral curves with low reflectance intensity in visible and infrared light. High concentrations of magnetite reduce the reflectance intensity of soils (Demattê et al., 2001) because magnetite does not show spectral features. At 1,400 and 1,900 nm, where features attributed to the OH^- of hygroscopic water occur (Ben-Dor, 2002), these soils have low intensity features. In the 2,200 nm wavelength region, a characteristic feature of 1:1 minerals appears, as indicated by Demattê and Garcia (1999).

The second group (Figure 4) consisted of soils with a textural B horizon typical of Argisols (Alfisols/Ultisols). We observed a gradual decrease of reflectance intensity from surface to subsurface layers, mainly because of the increase of clay content in deeper soil layers, in agreement with results observed by Sousa Junior et al. (2008). However, the spectral curve of the surface was significantly influenced by SOM, with consequent smoothing of the absorption features (Demattê and Garcia, 1999). In subsurface layers, there is more evidence of absorption bands within 1400 - 1900 nm because of the OH^- molecule of soil hygroscopic water (Ben-Dor, 2002) and the presence of 2:1 minerals (Demattê et al., 2004a). Thus, our results showed types of curves that differentiate soil samples from surface and subsurface layers, corroborating Demattê et al. (2004a), Rizzo et al (2014) and Vasques et al. (2014).

In the third and last group (Figure 4), sandy soils were joined, especially soils of the Quartzarenic Neosol class (Typic Quartzpisament). These soils are associated with lower contents of OM and iron oxides, with mineralogy in the sand fraction consisting predominantly of quartz (Resende et al., 2005), resulting in high reflectance intensity. This is evident when comparing the spectral curve of this group with that of group 1. This increase in reflectance was reported by Barnes and Baker (2000), who obtained high positive correlations between soil reflectance and increase in the sand fraction, and high negative correlations proportional to an increase in clay content. Another fact observed for patterns defined in group 3 is little distinction between spectral curves at different depths, which may be related to the textural similarity between soil layers (Souza Junior et al., 2008). However, layer A shows a slightly less intense reflectance than reflectance in the other layers because of greater OM accumulation.

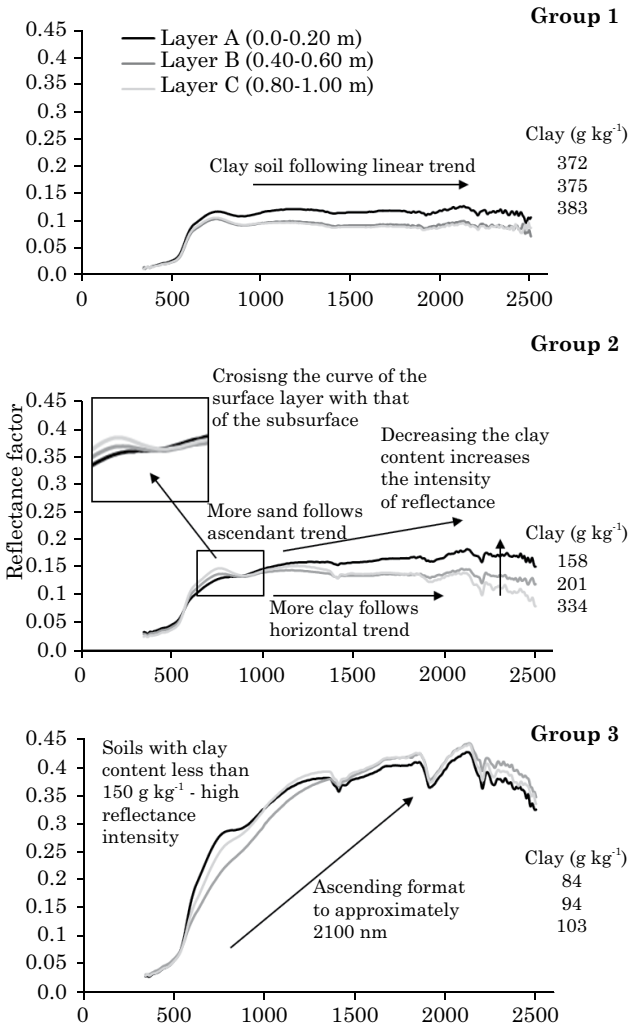

Figure 4. Clustering of soil samples as a function of the form of spectral curves. Group 1 - clayey soils, low reflectance; Group 2 - soils with difference of reflectance between the surface and subsurface layers, typical of horizon with Bt; Group 3 - sandy soil characteristics, high reflectance.

General characteristics of the Digital Soil Map (DSM) and comparison to the Conventional Map (CM)

The coverage area in the DSM is greater than in the CM (Table 3). The CM covers only sugarcane crop areas, thus bypassing roads, electrical lines, and other noncrop areas. However, this does not affect the correlation calculations between the maps because only areas in common were evaluated for both methods.

For soil classes in the 1st category level (orders), the DSM showed five classes, whereas the CM showed seven classes (Table 3). For Neossols (Lithic Neosols and Arenic Neosols), the 2nd category level was considered since the soils showed very distinct characteristics. Lithic Neossols and Gleysols were not covered in the DSM, although they showed a small index of representation in the CM (0.05 and 0.03 %, respectively).

In comparison to the CM, the DSM shows double the number of soil classes (43 classes). This is attributed to the absence of the aluminic character in digital classification. This method of soil analysis overestimated the dystrophic characteristic and underestimated the eutrophic and aluminic ones. This is most evident in the percentage of dystrophic soils

found; although they exhibited a high percentage in the CM (67 %), in the DSM, dystrophic soils reached 87 %.

Another relevant factor is that soils with a ferric character showed values near the significance level. Although the ferric property is a classification criterion in the 3rd category level, in conventional conditions, analyses of ferric properties are not often carried out, mainly due to the time required for the analysis and the high costs. This leads to the use of subjective methods of determination, such as magnetism. Analyses of ferric properties could be applied to samples from soils used in our study as well as in other conditions requiring less time to conduct and at lower costs.

From the confusion matrix generated by cross tabulation, some statistical indicators were analyzed to investigate the comparison between maps (Table 4). For point (punctual information) data, the variables of class, color, and texture showed better performance (good) compared to the variables of fertility and Fe (Table 4). The highest value for soil class shows that soil classification and determination of textural groups in the 1st category level were efficient, in agreement with Shepherd and Walsh (2002) and Islam et al. (2003). Color obtained a high index of success because it was obtained in the colorimetric technique (Campos and Demattê, 2004). These authors concluded that, in order to obtain accurate results, measurements in colorimetry should replace color readings using the visual Munsell color chart. Determining color by the human eye is subjective, generating differences in soil classification.

Fertility had poor performance (Table 4). The low *k* value is associated with the prevalence of this property. High prevalence results in a high level of agreement expected in randomness, which results in lower k values. In turn, a property of low prevalence results in higher k values (Pinto et al., 2007); that is, given that fertility shows high predominance of dystrophic soils and Fe has high predominance of non-ferric soils, there are high chances of inferring, at random, and being sure that these soils are dystrophic and non-ferric and that the *k* index results in lower values.

The results showed that spatial data had a tendency of high accuracy levels for the different variables analyzed individually (po ranging from 0.51 to 0.79), but, for texture, the performance of the kappa index ranged from good to reasonable.

The comparison between the classifications obtained for the two methods in the 1st, 2nd, and 3rd level (considering fertility), 3rd level (considering texture), and 3rd level (considering fertility plus texture) shows a good correlation of scores in the 1st and 2nd levels, with accuracy rates of 0.79 and 0.60, respectively, whereas for scores in the 3rd level, correlations ranged from reasonable to poor (Table 5). Higher levels were expected to decrease the accuracy rate because the greater the number of characters involved, the higher the difficulty in reaching consensus. However, the greatest losses of accuracy occur when associated with fertility.

The results for spatial data follow the same trends as point data, but with lower accuracy rates (Table 5). When fertility is inserted, the final mapping unit for this study is reached, with an accuracy rate of 0.08. Although fertility is difficult to assess, other variables such as class, color, and texture are subject to determination. If texture is taken as the 3rd level of classification, the results obtained are similar to those reported

Table 3. Comparisons among several characteristics observed in the digital and conventional soil maps

Characteristic	Conventional map	Digital map
Total area	12,986.92 ha	15,999.4 ha
Soil classes of 1st and 2nd levels (such as Neosols)(1)	Cambisols, Gleysols, Latossols (Oxisols), Nitisols (Kandic), Argisols (Ulti/Alfisols), Quartzarenic Neosols (Typic Quartzpisament), Lithic Neosols (Lithic soils)	Cambisols, Latossols (Oxisols), Nitisols (Kandic), Argisols (Ulti/Alfisols), Quartzarenic Neosols (Typic Quartzpisament)
Main soil classes	Latossols (Oxisols) (65.2 % of total area)	Latossols (Oxisols) (73.6 % of total area)
Less pronounced soil classes	Lithic Neosols (Lithic soils) (0.05 % of total area); Gleysols (0.03 % of total area)	Cambisols (0.17 % of total area)
Number of soil mapping units	43 units	21 units
Main soil mapping units[4]	LVAd4 (12.1 % of total area); RQod5 (11.6 % of total area)	LVAd3 (32 % of total area); RQod5 (12 % of total area)
Fertility classes	Eutrophic, Dystrophic, Aluminic	Eutrophic, Dystrophic
Main fertility class(1)	Dystrophic (67 % of total area)	Dystrophic (87 % of total area)
Area of ferric soils(1)	14 % of total area	11 % of total area
Textural groups(2)	Clayey, Sandy Clayey, Clayey Loamy, Sandy Loamy, Sandy	Sandy Clayey, Clayey Loamy, Sandy Loamy, Sandy
Main textural group	Clayey Loamy (38.1 % of total area)	Clayey Loamy (43 % of total area)

(1) Classes obtained according to criteria established by Embrapa (2013) as related with USDA (2010); (2) Texture divided into the following groups: 1 - clayey (>60 % clay); 2 - sandy clayey (35 - 60 % clay); 3 - clayey loamy (25 - 35 % clay); 4 - sandy loamy (15 - 25 % clay); and 5 - sandy (<15 % clay); (4) LVAd4 (Red Yellow Oxisol Distrophic sandy loam); RQod5 (Typic Quartzpisament), LVAd3 (Red Yellow Oxisol Distrophic clay loam).

by Demattê et al. (2004b). The authors concluded that it was possible to reach the 3rd category level. Chagas et al. (2007) used artificial neural networks to predict soil classes and found accuracy rates of 0.3. The authors attributed the large discrepancy obtained for the comparisons to the widespread nature of the conventional soil map. The multiple information from geotechnologies on soil mapping was recently conducted by Demattê et al. (2015) where used also spectra from images plus terrain models reaching important results when compared with traditional mapping, in agreement with the present work. Another important factor is that accuracy and effectiveness of surveys conducted conventionally are contingent upon the ability of the pedologist. Indeed Basaglia Filho et al. (2013) showed differences in maps developed between five pedologists, which show the importance of increasing accuracy through geotechnologies, as indicated in the present study.

Thus, the present manuscript associated with literature, indicate the importance on to aggregate multiple techniques, such as remote/proximal sensing with relief parameters, to achieve a pedological map. Indeed, these tools may also be important to upgrade old maps and/or on the confection of new ones with more accuracy, less time and lower cost.

Table 4. Statistical indexes derived from confusion matrix between point results (bore holes) and spatial results (soil maps) obtained by crossing five variables between the conventional and the digital soil map

Variable	Statistical Indexes (1)					Performance(2)
	po	pe	Kappa	Var (k)	Z	
			Point data			
Class	0.79	0.59	0.49	0.0021	10.7	Good
Color	0.72	0.48	0.46	0.0041	7.2	Good
Fertility	0.69	0.65	0.12	0.0015	3.1	Bad
Iron	0.80	0.76	0.14	0.0050	7.0	Good
Texture	0.58	0.29	0.41	0.0017	9.8	Good
			Spatial data			
Class	0.75	0.59	0.39	0.0000	60.40	Good
Color	0.72	0.47	0.47	0.0000	50.83	Good
Fertility	0.70	0.68	0.05	0.0000	13.40	Bad
Iron	0.79	0.76	0.12	0.0001	50.00	Good
Texture	0.51	0.26	0.34	0.0030	6.30	Reasonable

(1) po: total accuracy or real concordance; pe: random concordance; Kappa: kappa index; var (k): variance of kappa index; Z: statistical index to test the significance of kappa index: If Z>1.96, difference is significant at 95 % confidence threshold; if Z>2.58, difference is significant at 99 % confidence threshold. (2) Classification in the kappa index.

Table 5. Statistical index derived from the confusion matrix between the point results (boreholes with auger) and spatial results (soil map) obtained by crossing soil taxonomy in the 1st, 2nd, and 3rd levels considering fertility, the 3rd level considering texture, and the 3rd level considering fertility plus texture

Variable	Statistical Indexes(1)					Performance(2)
	po	pe	Kappa	Var (k)	Z	
			Point data			
1º Level	0.79	0.59	0.49	0.00	10.69	Good
2º Level	0.60	0.27	0.45	0.00	12.10	Good
3º Level (fertility)	0.37	0.16	0.25	0.00	9.62	Bad
3º Level (texture)	0.40	0.12	0.32	0.00	13.00	Reasonable
3º Level (fertility + texture)	0.20	0.06	0.15	0.00	7.00	Bad
			Spatial data			
1º Level	0.75	0.59	0.39	0.00	60.40	Good
2º Level	0.60	0.27	0.45	0.00	14.46	Good
3º Level (fertility)	0.21	0.09	0.14	0.00	9.20	Bad
3º Level (texture)	0.34	0.11	0.26	0.00	82.47	Reasonable
3º Level (fertility + texture)	0.08	0.03	0.05	0.00	31.26	Bad

(1) po: total accuracy or real concordance; pe: random concordance; Kappa: kappa index; var (k): variance of kappa index; Z: statistical index to test the significance of the kappa index: If Z>1.96, difference is significant at 95 % confidence threshold; If Z>2.58, the difference is significant at 99 % confidence threshold. (2) Classification in the kappa index.

CONCLUSIONS

The spectral curve patterns allowed determination of three distinct soil groups, namely: (a) clayey in the surface and subsurface soils, (b) soils with textural differences between depths (typical of soils with Bt horizon), and (c) sandy soils.

The method for quantification of attributes such as Al^{3+}, CEC, base and aluminum saturation needs to be adjusted or modified to reliably achieve the 3rd category level in soil classification. However, for properties such as clay, sand, Fe_2O_3, and Al_2O_3, the method was efficient, with R^2 of 0.75, 0.71, 0.82, and 0.81, respectively.

The proposed method obtained information that assisted in soil classification and mapping in the 1st category level with 75 % accuracy, in the 2nd category level with 60 % accuracy, and in the 3rd category level with 34 % accuracy considering texture for the 3rd level. The performance of classification was good in the 2nd category level and reasonable when information on soil texture is added to it. Furthermore, when fertility is considered, the accuracy index reaches 8 %.

The comparison of five textural groups between both conventional and digital methods reached 58 % accuracy.

There is clear importance of soil spectroscopy (from the surface and subsurface) on soil discrimination. Soil surface information from the satellite was useful for a first view on the discrimination of surface data. The next step was to achieve undersurface spectroscopy data from samples collected at field. Afterwards, both surface (by remote sensing) and subsurface (by proximal sensing) information, merged with relief parameters, could provide the method with important results as to support pedological mapping.

We observed the importance of using multiple techniques simultaneously to support soil mapping. Nevertheless, the method still requires the interpreter's knowledge in making the final decision. Fieldwork is also important because it is the basis for designing patterns, as well as for defining situations where digital techniques do not reach adequate levels. Further studies are suggested as to associate field observations with automated systems for the decision-making process.

ACKNOWLEDEGMENT

Authors thank GeoSS (Geotechnologies in Soil Science Group, http://esalqgeocis.wix.com/english).

REFERENCES

Antunes MAH, Freire RMB, Botelho AS, Toniolli LH. Correções atmosféricas de imagens de satélites utilizando o modelo 6S. In: Anais do 21º Congresso Brasileiro de Cartografia; 2003; Belo Horizonte. Rio de Janeiro: Sociedade Brasileira de Cartografia; 2003.

Barnes EM, Baker MG. Multispectral data for mapping soil texture: possibilities and limitations. Appl Eng Agric. 2000;16:731-41.

Bazaglia Filho O, Rizzo R, Lepsch IF, Prado H, Gomes FH, Mazza JÁ, Demattê JAM. Comparison between detailed digital and conventional soil maps of an area with complex geology. R Bras Ci Solo. 2013;37:1136-48.

Bellinaso H, Demattê JAM, Araujo SR. Spectral library and its use in soil classification. R Bras Ci Solo. 2010;34:861-70.

Ben-Dor E. Quantitative remote sensing of soil properties. Adv Agron. 2002;75:173-243.

Bistrichi CA, Carneiro CDR, Dantas ASL, Ponçano WL, Campanha GAC, Nagata N, Almeida MA, Stein DP, Melo MS, Cremonini OA. Mapa geológico do Estado de São Paulo. São Paulo: Instituto de Pesquisas Tecnológicas do Estado de São Paulo - IPT; 1981. 1 mapa, Escala: 1:500.000.

Brown DJ, Shepherd KD, Walsh MG, Mays MD, Reinsch TG. Global soil characterization with VNIR diffuse reflectance spectroscopy. Geoderma. 2006;132:273-90.

Camargo AO, Moniz AC, Jorge JA, Valadares JMAS. Métodos de análise química, mineralógica e física de solos. Bol Tec Inst Agron. 1986;106:1-94.

Campos RC, Demattê JAM. Cor do solo: uma abordagem da forma convencional de obtenção em oposição à automatização do método para fins de classificação de solos. R Bras Ci Solo. 2004;28:853-63.

Chagas CS, Fernandes Filho EI, Vieira CAO, Carvalho Júnior W. Utilização de redes neurais artificiais para predição de classes de solo em uma bacia hidrográfica no Domínio de Mar de Morros. In: Anais do 13º Simpósio Brasileiro de Sensoriamento Remoto; 2007; Florianópolis. Florianópolis: Sociedade Brasileira de Sensoriamento Remoto; 2007. p.2421-8.

Chang C, Laird DA, Mausbach MJ, Hurburgh Junior CR. Near-Infrared reflectance spectroscopy - principal components regression analyses of soil properties. Soil Sci Soc Am J. 2001;65:480-90.

Congalton RG, Green K. Assessing the accuracy of remotely sensed data: principles and practices. NewYork: Lewis Publishers; 1999.

Crósta AP. Processamento digital de imagens de sensoriamento remoto. Campinas: Universidade Estadual de Campinas; 1992.

Deering DW, Rouse JW, Haas RH, Schell JA. Measuring "forage production" of grazing units from Landsat MSS data. In: Proceedings of the 10º International Symposium on Remote Sensing of Environment; 1975; Ann Arbor. Ann Arbor, MI: ERIM, 1975. v.2, p.1169-78.

Demattê JAM, Alves MR, Gallo BC, Fongaro CT, Romero DJ, Sato MV. Hyperspectral remote sensing as an alternative to estimate soil attributes. R Ci Agron. 2014a;46:223-32.

Demattê JAM, Bellinaso H, Romero DJ, Fongaro CT. Morphological Interpretation of Reflectance Spectrum (MIRS) using libraries looking towards soil classification. Sci Agric. 2014b;71:509-20.

Demattê JAM, Campos RC, Alves MC, Fiorio PR, Nanni M. R.Visible-NIR reflectance: a new approach on soil evaluation. Geoderma. 2004b;121:95-112.

Demattê JAM, Demattê JLI, Camargo WP, Fiorio PR, Nanni MR. Remote sensing in the recognition and mapping of tropical soils developed on topographic sequences. Mapp Sci Rem Sens. 2001;38:79-102.

Demattê JAM, Fiorio P, Campos RC, Nanni M, Costa Lima JC, Costa Lima WC. Soil Survey scale and its effects on land use planning. Mapp Sci Rem Sens. 2002;39:258-72.

Demattê JAM, Fiorio PR, Ben-Dor E. Estimation of soil properties by orbital and laboratory reflectance means and its relation with soil classification. Open Rem Sens J. 2:12-23, 2009.

Demattê JAM, Garcia GJ. Alteration of soil properties through a weathering sequence as evaluated by spectral reflectance. Soil Sci Soc Am J. 1999;63:327-42.

Demattê JAM, Genú AM, Fiorio PR, Ortiz JL, Mazza JA, Leonardo HCL. Comparação entre mapas de solos obtidos por sensoriamento remoto espectral e pelo método convencional. Pesq Agropec Bras. 2004a;39:1219-29.

Demattê JAM, Rizzo R, Botteon VW. Pedological mapping through integration of digital terrain models spectral sensing and photopedology. R Ci Agron. 2015;46:669-78.

Dobos E, Micheli E, Baumgardner MF, Biehl L, Helt T. Use of combined digital elevation model and satellite radiometric data for regional soil mapping. Geoderma. 2000;97:367-91.

Dunn BW, Beecher HG, Batten GD, Ciavarella S. The potential of near-infrared reflectance spectroscopy for soil analysis - a case study from the Riverine Plain of south-eastern Australia. Aust J Exp Agric. 2002;42:607-14.

Empresa Brasileira de Pesquisa Agropecuária - Embrapa. Sistema brasileiro de classificação de solos. 3ª.ed. Brasília, DF: 2013.

Fiorio PR, Demattê JAM, Nanni MR, Genú AM, Martins JA. In situ separation of soil types along transects employing Vis-NIR sensors: a new view of soil evaluation. R Ci Agron. 2014;45:433-42.

Fonseca LMG. Processamento digital de imagens. São José dos Campos: Instituto Nacional de Pesquisas Espaciais; 2000.

Franceschini MHD, Demattê JAM, Sato MV, Vicente LE, Grego CR. Abordagens semiquantitativa e quantitativa na avaliação da textura do solo por espectroscopia de reflectância bidirecional no VIS-NIR-SWIR. Pesq Agropec Bras. 2013;48:1568-81.

Gessler PE, Moore ID, Mckenzie NJ, Ryan PJ. Soil-landscape modeling and spatial prediction of soil attributes. Integrating GIS and environmental modeling. Int J Geogr Inform Syst. 1995;9:421-32. (Special issue)

Glantz SA, Slinker BK. Primer of applied regression and analysis of variance. New York: MacGraw-Hill Book; 1990.

Islam K, Singh B, Mcbratney AB. Simultaneous estimation of several soil properties by ultra-violet, visible, and near-infrared reflectance spectroscopy. Aust J Soil Res. 2003;41:1101-14.

Jackson TJ, Schmugge J, Engman ET. Remote sensing applications to hydrology: soil moisture. Hydrol Sci J. 1996;41:517-30.

Janik LJ, Merry RH, Skjemstad JO. Can mid infrared diffuse reflectance analysis replace soil extractions? Aust J Exp Agric. 1998;38:681-96.

Kobayashi K, Salam MU. Comparing simulated and measured values using mean squared deviation and its components. Agron J. 2000;92:345-52.

Mcbratney AB, Mendonça Santos ML, Minasny B. On digital soil mapping. Geoderma. 2003;117:3-52.

Mckenzie NJ, Gessler PE, Ryan PJ, O'connell DA. The role of terrain analysis in soil mapping. In: Wilson JP, Gallant JC, editors. Terrain analysis: principles and applications. New York: John Wiley; 2000. p. 245-65.

Metternicht GI, Zinck JA. Remote sensing of soil salinity: potentials and constraints. Rem Sens Environ. 2003;85:1-20.

Milne G. Some suggested units of classification and mapping particularly for East African soils. Soil Res. 1935;4:183-98.

Mitishita EA, Kirchner FP, Andrade JB. Transformação de entidades naturais e artificiais para o sistema cartográfico, obtidas a partir de imagens digitais de satélite. In: Anais do 5º Simpósio Brasileiro de Sensoriamento Remoto; 1988; Natal. São José dos Campos: INPE; 1988. p.497-502.

Moore ID, Gessler PE, Nielson GA. Soil attribute prediction using terrain analysis. Soil Sci Soc Am J. 1993;57:443-52.

Nanni MR, Demattê JAM. Spectral methodology in comparison to traditional soil analysis. Soil Sci Soc Am J. 2006;70:393-407.

Nanni MR, Demattê JAM. It is possible to estimate physical-chemical soil attributes by using laboratory and orbital sensors. In: Proceedings of the 3rd. International Conference of Geospatial Information in Agriculture and Forestry [CD ROM]; 2001; Denver. Denver: Veridian; 2001.

Odeh IOA, Mcbratney AB. Using AVHRR images for spatial prediction of clay content in the lower Namoi Valley of eastern Australia. Geoderma. 2000;97:237-54.

Oliveira VA. O Brasil carece de novos pedólogos. Bol Inf. Soc Bras Ci Solo. 1999;25:25-8.

Pinto JS, Lopes JM, Oliveira JV, Amaro JP, Costa LD. Métodos para estimação de reprodutividade de medidas. [Accessed: 2007 Nov. 15]. Available at: http://users.med.up.pt/joakim/intromed/estatisticakappa.htm.

Research Systems - RSI. The Environment for Visualizing Images - ENVI. Boulder: 2006.

Resende M, Curi N, Ker JC, Rezende SB. Mineralogia de solos brasileiros: interpretação e aplicações. Lavras: Universidade Federal de Lavras; 2005.

Rizzo R, Demattê JAM, Terra FS. Using numerical classification of profiles based on Vis-Nir spectra to distinguish soils from the Piracicaba region, Brazil. R Bras Ci Solo. 2014;38:372-85.

Rodrigues TRI, Rocha AM, Perez Filho A. Mapeamento de uso e ocupação das terras na Bacia do Baixo Curso do Rio São José do Dourados-SP por sistemas de informações geográficas e imagem de satélite. In: Anais do 13º Simpósio Brasileiro de Sensoriamento Remoto [CD ROM]; 2007; Florianópolis. São José dos Campos: INPE; 2007. p. 6091-7.

Rossiter D. Digital soil mapping: towards a multiple-use soil information system. Anal Geogr. 2005;32:7-15.

Rouse JW Jr, Haas RH, Deering DW, Schell JA, Harlan JC. Monitoring the vernal advancement and retrogradation (green wave effect) of natural vegetation [Type III Final Report]. Greenbelt: NASA/GSFC; 1974.

Santos HG. Importância e evolução dos levantamentos de solos no Brasil. Bol Inf Soc Bras Ci Solo. 2007;32:21-6.

Savitzky A, Golay MJE. Smoothing and differentiation of data by simplified least squares procedures. Anal Chem. 1964;36:1627-39.

Shary PA, Sharayab LS, Mitusov AV. Fundamental quantitative methods of land surface analysis. Geoderma. 2002;107:1-32.

Shepherd KD, Walsh MG. Development of reflectance spectral libraries for characterization of soil properties. Soil Sci Soc Am J. 2002;66:988-98.

Shimabukuro YE, Smith JA. The least-squares mixing models to generate fraction images derived from remote sensing multispectral data. IEEE Trans Geosci Rem Sens. 1991;29:16-20.

Sneath PHA, Sokal RR. Numerical taxonomy. San Francisco: W. H. Freemam; 1973.

Sousa Junior JGA, Demattê JAM, Genu AM. Comportamento espectral dos solos na paisagem a partir de dados coletados por sensores terrestre e orbital. R Bras Ci Solo. 2008;32:727-38.

Stein A, Bastiaanssen WGM, De Bruin S, Cracknell AP, Curran PJ, Fabbri AG, Gorte BGH, van Groenigen JW, van der Meer FD, Saldaña A. Integrating spatial statistics and remote sensing. Int J Rem Sens. 1998;19:1793-814.

Story M, Congalton RG. Accuracy assessment: A user's perspective. Photogram Eng Remote Sens. 1986;52:397-9.

United States Department of Agriculture - USDA. [Accessed: 2010 Dec. 12]. Available at: http://www.soils.usda.gov/technical/handbook/contents/part630.html.

Vasques GM, Demattê JAM, Ramírez-López L, Terra FS. Soil classification using visible/near-infrared diffuse reflectance spectra from multiple depths. Geoderma. 2014;223:73-8.

Vermote EF, Tanré D, Deuzi JL, Herman M, Morcrette JJ. Second simulation of the satellite signal in the solar spectrum, 6S: An overview. IEEE Trans Geosci Rem Sens. 1997;35:675-86.

Wolschick D, Martinez MA, Fontes PCR, Matos AT. Implementação e teste de um modelo mecanístico de simulação do crescimento e desenvolvimento de plantas de milho. R Bras Eng Agríc Amb. 2007;11:271-8.